Hindawi
Andrologia
Volume 2023, Article ID 5488279, 13 pages
https://doi.org/10.1155/2023/5488279

Research Article

Extracellular Matrix and Protein Phosphorylation Dysregulation Related to Diabetes-Induced Erectile Dysfunction

Zhiguo Zhu,[1,2,3] **Xiaoli Li**,[4] **Xiande Cao**,[1] **Huisheng Qin**,[1] **Dong Yue**,[1] **Deqian Liu**,[1] **Guigeng Tan**,[1] **Xujun Xuan**,[3] **and Haizhou Zhu**[1]

[1]*Department of Urology, Affiliated Hospital of Jining Medical University, Jining Medical University, Jining, Shandong, China*
[2]*Postdoctoral Mobile Station of Shandong University of Traditional Chinese Medicine, Jining, Shandong, China*
[3]*Department of Andrology, The Seventh Affiliated Hospital Sun Yet-sen University, Shenzhen, Guangdong, China*
[4]*Department of Outpatient Office & Outpatient Operating Room, The Seventh Affiliated Hospital Sun Yet-sen University, Shenzhen, Guangdong, China*

Correspondence should be addressed to Xujun Xuan; xuanxujun@sysush.com and Haizhou Zhu; profzhuhz@163.com

Received 18 October 2022; Revised 22 February 2023; Accepted 17 March 2023; Published 1 April 2023

Academic Editor: Debarshi Sarkar

Copyright © 2023 Zhiguo Zhu et al. This is an open access article distributed under the Creative Commons Attribution License, which permits unrestricted use, distribution, and reproduction in any medium, provided the original work is properly cited.

Diabetes can cause erectile dysfunction (ED) in more than half of male patients. However, the mechanisms underlying diabetes-induced erectile dysfunction (DED) remain unknown. This study is aimed at systematically analyzing the cellular and molecular mechanisms leading to DED using bioinformatic analysis and providing molecular targets for predicting and treating DED. In total, we identified 800 DEGs in the DED samples compared with those in the control group. The 407 upregulated DEGs were mainly enriched in glucose and lipid metabolism-related pathways, and the 393 downregulated DEGs were primarily enriched in tissue development and structure. Dysregulated extracellular matrix genes (especially collagen and elastin) may be closely related to damage to the erectile function of the corpus cavernosum. Sixteen hub genes and 24 modules were detected with hub genes and MCODE analysis. The consensus sequence AAA (G/C) AAA was observed at the promoter sites of most genes that were enriched in the "posttranslational protein phosphorylation" pathway. These genes had abundant phosphorylation sites. Furthermore, 20 TFs targeting DEGs were identified using ChEA3 tool. In conclusion, our research comprehensively and systematically describes the molecular characteristics of DED and suggests that dysregulated extracellular matrix genes and protein phosphorylation may play critical roles in DED. Therefore, they may be potential markers for diagnosing and treating DED.

1. Introduction

Diabetes mellitus is a chronic, noncommunicable disease associated with multiple organ and system complications [1]. In recent decades, the global incidence of adult diabetes has increased at an accelerated growth rate. The number of patients with diabetes aged 20-79 years is expected to increase to 642 million by 2040 [2]. Diabetes can cause several health problems, including sexual dysfunction [3]. In male patients, sexual dysfunction is mainly manifested as erectile dysfunction (ED), with a global prevalence of 52.5% (type I diabetes, 37.5%; type II diabetes, 66.3%) [4]. Due to the high incidence of type II diabetes mellitus (T2DM), research on diabetes-induced ED has also focused on T2DM. However, T1DM incidence is increasing worldwide, and the reasons for this are incompletely understood [5]. T1DM-induced ED should also receive the attention of researchers. Therefore, we conducted this study to determine the molecular features of T1DM-induced ED.

The etiology of diabetic erectile dysfunction (DED) is complicated and may be related to endothelial dysfunction, smooth muscle injury, vascular disease, neuropathy, abnormal hormone levels, inflammation, and cavernous fibrosis [6]. DED has always been a challenge for endocrinologists and urologists, who have used oral phosphodiesterase type 5 inhibitors (PDE5i) as the first-line treatment for ED, including DED. However, DED is often resistant to PDE5i treatment [7]. Intracavernous administration of vasoactive

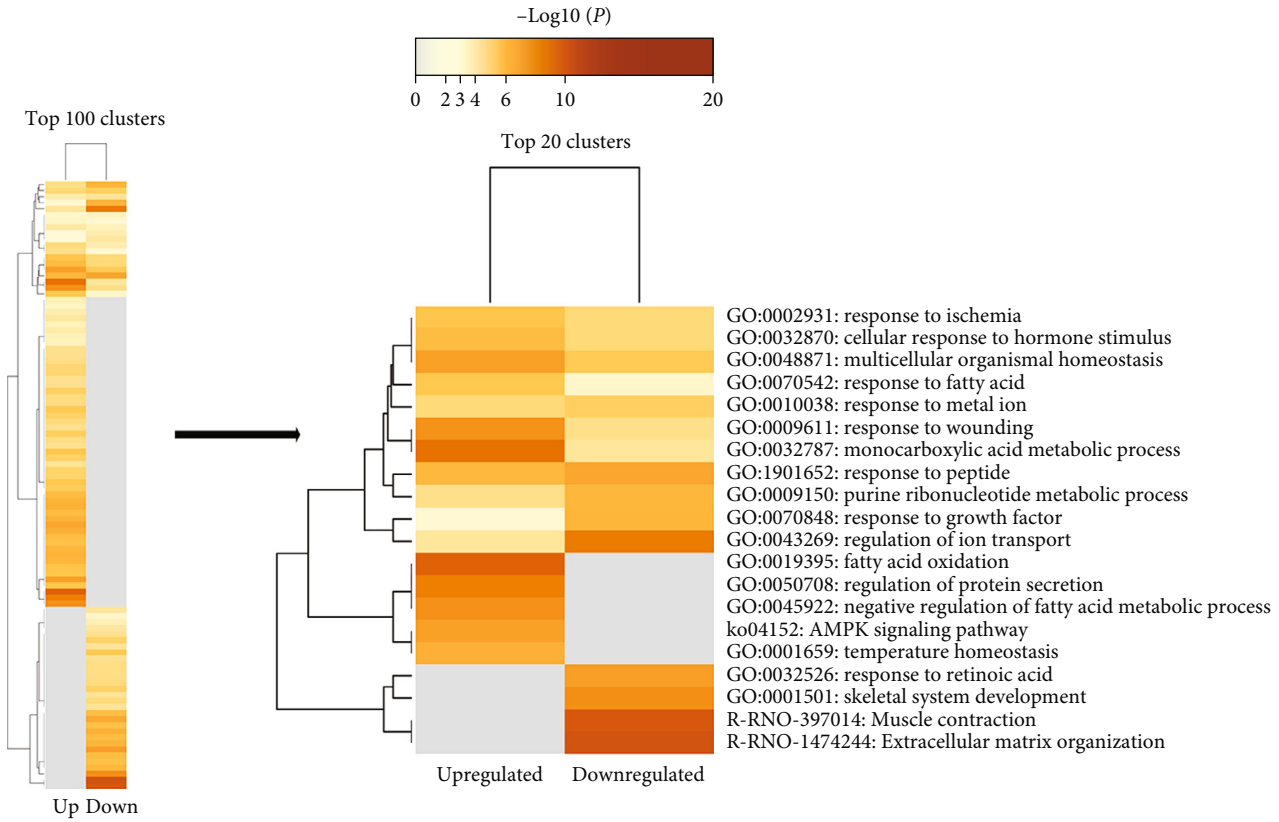

Figure 1: Heatmap of enriched terms across input gene lists.

drugs, commonly used as a second-line medical treatment when PDE5i fails, often induces unavoidable complications, including penile pain, hydrocephalus, priapism, and fibrosis [7]. Consequently, patients often choose to undergo penile prosthesis implantation. Therefore, although great progress has been made in recent decades, medical treatment for DED remains difficult [8]. In addition, many studies have evaluated the mechanism of DED [9–12], but there is a lack of understanding at the cellular and molecular levels.

Here, we systematically analyzed the molecular correlates of ED in diabetes using bioinformatics. Differentially expressed genes (DEGs) were identified in a diabetes-induced ED rat model. We analyzed the function and interaction pathways of the DEGs and performed hub gene and module analyses. Conserved motifs in the promoter regions and their posttranslational phosphorylation modifications were studied. In addition, we searched for transcription factors (TFs) that may target DEGs.

2. Materials and Methods

2.1. Data Collection. We used "diabetes" and "erectile dysfunction" to search the Gene Expression Omnibus (GEO) database (https://www.ncbi.nlm.nih.gov/geo/) and selected the GSE2457 gene expression dataset for the next analysis [13]. Considering the ethical principles and difficulty of obtaining penile tissue samples from patients with DED, microarray experiments were performed on the cavernous tissue of a diabetes-induced ED rat model. In their study, the two-month rats were intraperitoneally injected with 35 mg streptozotocin (STZ) per kg body weight in sterile citrate buffer to induce diabetes. The body weight and glucose levels of each animal were monitored weekly over the course of the study (10 weeks). Diabetes is a blood glucose level of >300 mg/dL. The response of intracavernous pressure (ICP) to cavernous nerve stimulation was measured ten weeks after the induction of diabetes in all rats. Finally, blood glucose was significantly higher in diabetic rats than in control rats (386 ± 8 vs. 94 ± 5 mg/dL, $P < 0.0001$), and glucose levels in the STZ group were maintained at 300 mg/dL or above throughout the course of the study. The mean ΔICP/MAP was lower at all voltages in the diabetic rats than in the controls. More detailed information can be found in PMID: 16118269.

2.2. Identification of Differentially Expressed Genes. GEO2R tool (https://www.ncbi.nlm.nih.gov/geo/geo2r/) was used to extract differentially expressed genes (DEGs). $P < 0.05$ and fold change > 1.5 (or <0.67) were chosen as the cutoff criteria.

2.3. Gene Annotation and Enrichment Analysis of DEGs. Metascape (http://metascape.org) is a web-based tool that can provide automated gene list annotation and enrichment analysis [14]. Enrichment analysis was based on the following ontology sources: Gene Ontology (GO) processes, KEGG pathways, canonical pathways, Reactome gene

Table 1: Top 20 clusters with their representative enriched terms.

Gene list	Terms	Category	Description	Count	%	Log10 (*P*)	Log10 (*q*)
■	R-RNO-1474244	Reactome gene sets	Extracellular matrix organization	24	6.78	-11.15	-6.90
■■	GO:0032787	GO biological processes	Monocarboxylic acid metabolic process	61	8.43	-10.44	-6.16
■	R-RNO-397014	Reactome gene sets	Muscle contraction	20	5.65	-10.23	-6.90
■■	GO:1901652	GO biological processes	Response to peptide	63	8.70	-9.72	-5.74
■■	GO:0043269	GO biological processes	Regulation of ion transport	68	9.39	-9.36	-5.74
■	GO:0019395	GO biological processes	Fatty acid oxidation	16	4.31	-9.27	-6.06
■■	GO:0048871	GO biological processes	Multicellular organismal homeostasis	53	7.32	-9.25	-5.74
■■	GO:0009611	GO biological processes	Response to wounding	61	8.43	-9.05	-5.73
■	GO:0050708	GO biological processes	Regulation of protein secretion	28	7.55	-7.56	-4.84
■■	GO:0032870	GO biological processes	Cellular response to hormone stimulus	64	8.84	-7.51	-4.65
■■	GO:0009150	GO biological processes	Purine ribonucleotide metabolic process	45	6.22	-7.47	-4.63
■■	GO:0002931	GO biological processes	Response to ischemia	15	2.07	-7.31	-4.52
■	ko04152	KEGG pathway	AMPK signaling pathway	20	2.76	-7.02	-4.33
■	GO:0001501	GO biological processes	Skeletal system development	30	8.47	-6.70	-4.12
■	GO:0045922	GO biological processes	Negative regulation of fatty acid metabolic process	8	2.16	-6.63	-4.10
■■	GO:0010038	GO biological processes	Response to metal ion	45	6.22	-6.34	-3.84
■■	GO:0070848	GO biological processes	Response to growth factor	60	8.29	-5.97	-3.54
■	GO:0032526	GO biological processes	Response to retinoic acid	14	3.95	-5.92	-3.54
■■	GO:0070542	GO biological processes	Response to fatty acid	19	2.62	-5.87	-3.47
■	GO:0001659	GO biological processes	Temperature homeostasis	23	3.18	-5.78	-3.39

Abbreviations: ■: upregulated genes; ■: downregulated genes; GO: Gene Ontology; KEGG: Kyoto Encyclopedia of Genes and Genomes; AMPK: adenosine 5′-monophosphate-activated protein kinase.

sets, PaGenBase, and CORUM. In addition, we used this tool to produce a heatmap and network of enriched terms.

2.4. PPI Network, Hub Gene, and Module Analysis. The Search Tool for the Retrieval of Interacting Genes (STRING, https://string-db.org/) was applied to detect the interactions of the DEGs and construct the PPI network [15]. Cytoscape software was used to optimize the PPI network [16]. Two Cytoscape software plug-ins, cytoHubba and Molecular Complex Detection (MCODE), were used to identify the hub genes and screen modules of the PPI network.

2.5. Identification of Conserved Motifs in Promoter Site. Ensembl (https://ensembl.org/) was used to obtain the promoter site (2000 bp upstream of the transcription start site) [17]. Gapped Local Alignment of Motifs (GLAM2) was used to discover common conserved motifs in the gene of interest [18].

2.6. Prediction of the Phosphorylation Sites. Protein sequences were retrieved from the National Center for Biotechnology Information website (https://www.ncbi.nlm.nih.gov/protein). NetPhos 3.1 server (http://www.cbs.dtu.dk/services/NetPhos/) was used to predict serine, threonine, and tyrosine phosphorylation sites in the selected proteins [19].

2.7. Prediction of TFs Associated with DEGs. ChEA3 (https://maayanlab.cloud/chea3/) is an online tool that can be used for transcription factor (TF) enrichment analysis by orthogonal omics integration [20]. We used this tool to identify TFs that target DEGs.

2.8. Statistical Analysis. All statistical analyses were conducted using SPSS version 20.0 (SPSS Inc., Chicago, IL, USA) and GraphPad Prism version 8.0 (GraphPad Software, San Diego, CA, USA). $P < 0.05$ indicated statistical significance.

3. Results

3.1. Identification and Enrichment Analysis of DEGs. The array analysis was based on $a > 1.5$ (or <0.67)-fold change in expression and $P < 0.05$. According to these criteria,

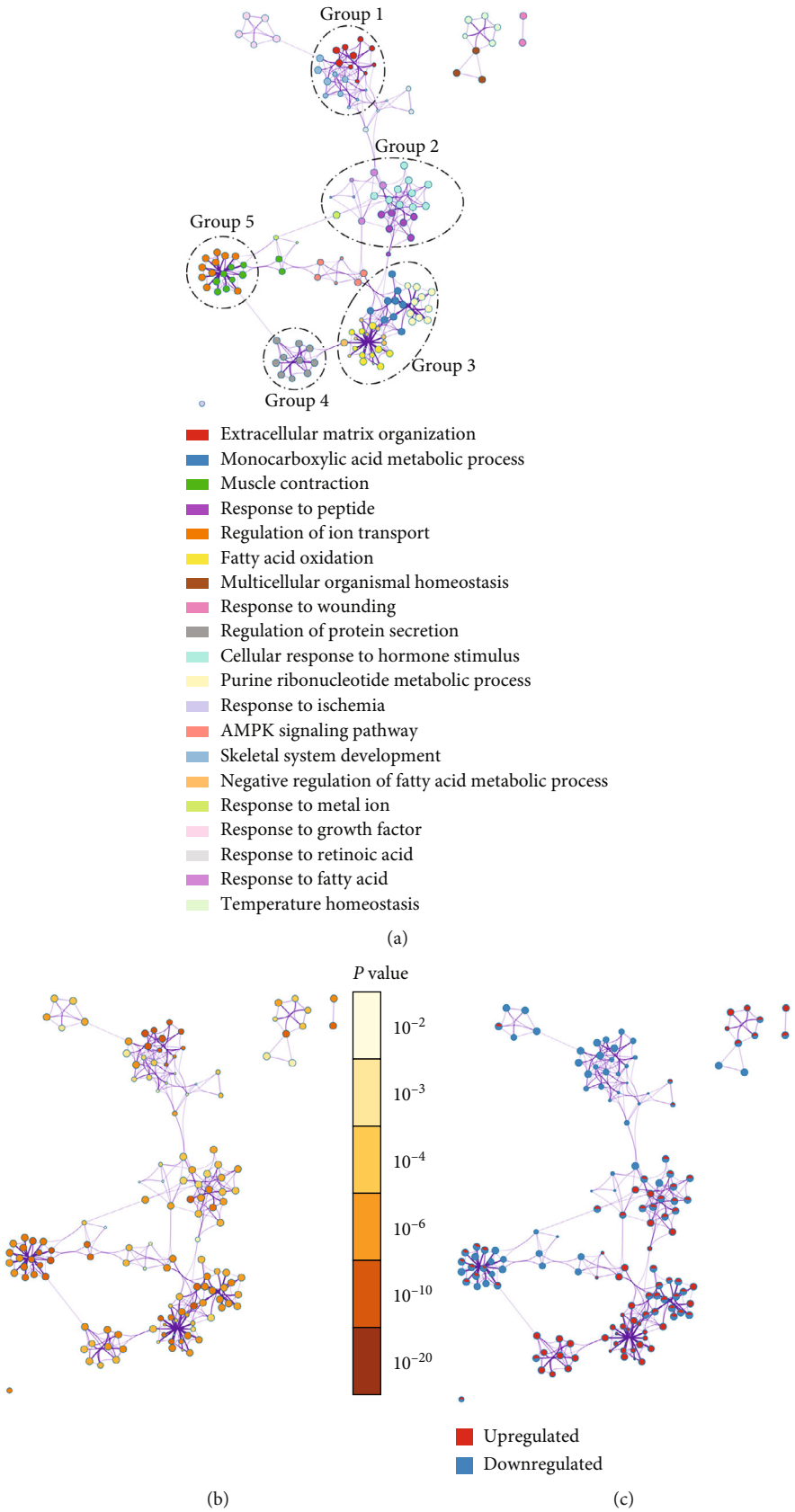

Figure 2: Visualizations of functional enrichment and interactome analysis results of the DEGs. Network of enriched terms: (a) colored by enriched terms and five groups formed; (b) colored by the *P* value; (c) color-coded based on the identities of the gene lists. Abbreviations: DEGs: differentially expressed genes; GO: Gene Ontology; AMPK: adenosine 5′-monophosphate-activated protein kinase.

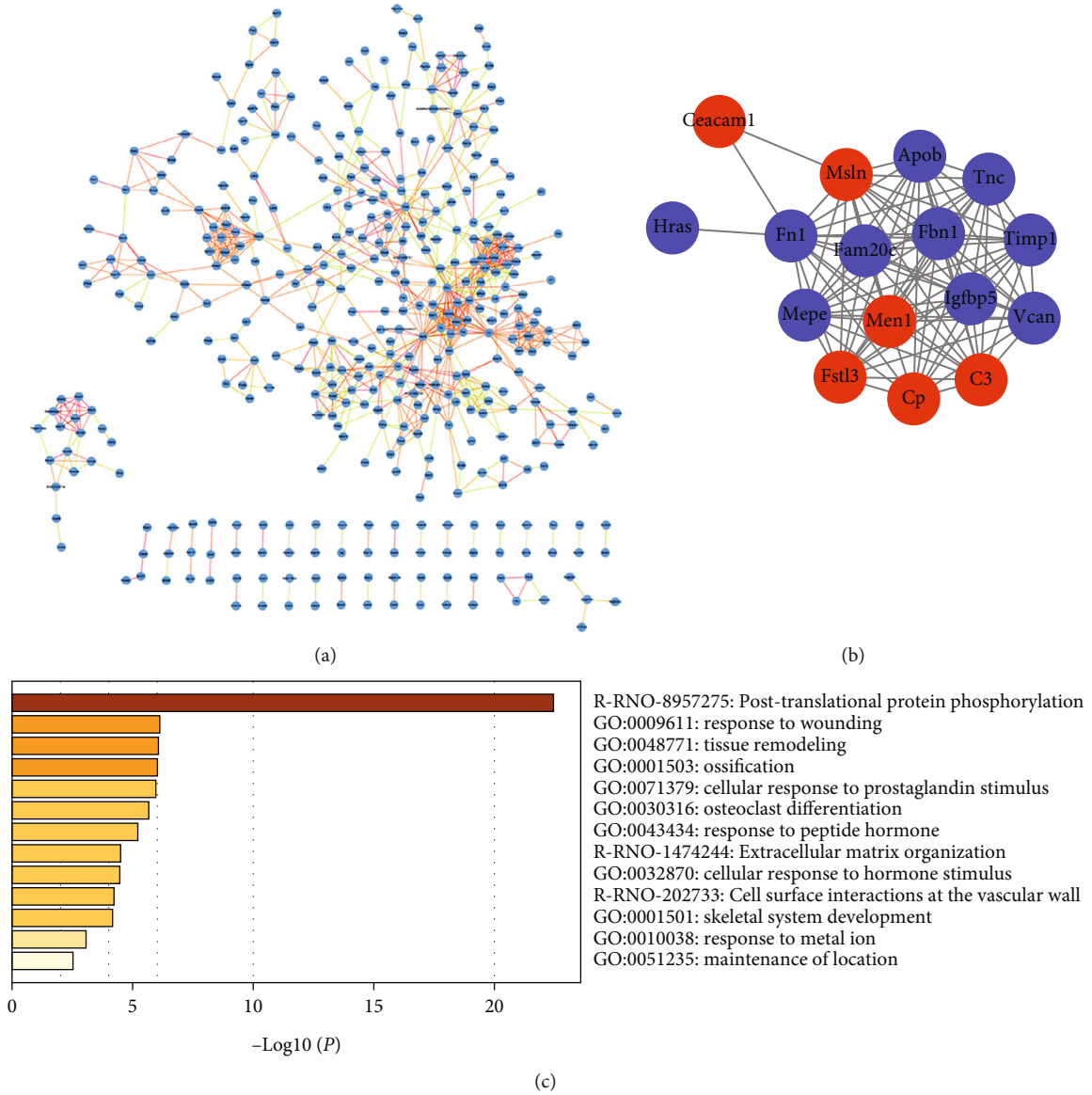

Figure 3: (a) PPI network of the DEGs. The edge color reflects the combined score of the genes (green→red = low score→high score). (b) PPI network of 16 hub genes and enrichment analysis of these genes (c). Abbreviations: DEGs: differentially expressed genes; GO: Gene Ontology; PPI: protein-protein interaction.

800 DEGs (407 upregulated and 393 downregulated) were detected (Table S1).

We used Metascape to perform annotation and enrichment analyses of these genes. Figure 1 displays the Metascape enrichment analysis results as a clustered heatmap. In the top 100 enriched clusters (Figure S1), the upregulated and downregulated genes were mostly different, and only a small portion of the results overlapped. When the results were limited to the top 20 clusters, the overlap probability of enrichment results increased. However, the main functions of the upregulated and downregulated genes differed significantly. The upregulated DEGs were enriched in glucose and lipid metabolism-related pathways: "fatty acid oxidation", "monocarboxylic acid metabolic process", "negative regulation of fatty acid metabolic process", and "AMPK signaling pathway". The downregulated DEGs were primarily enriched in tissue development and structure: "extracellular matrix organization", "muscle contraction", and "skeletal system development". Table 1 illustrates the top 20 clusters with their representative enriched terms, the number of genes enriched in each term, and the percentage of genes that are found in the given ontology term.

We built an enrichment network to demonstrate the relationships between the top 20 terms. In the network, each node represented an enriched cluster and was first colored by its cluster ID (Figure 2(a)) and then by its P value (Figure 2(b)). From the network, there were mainly five-term groups formed: group 1: "extracellular matrix organization" and "skeletal system development"; group 2: "response to peptide," "cellular response to hormone stimulus," and "response to fatty acid"; group 3: "monocarboxylic acid

Table 2: Top 20 hub genes detected using the 12 algorithms in cytoHubba plug-in.

Rank	Algorithms											
	MCC	DNMC	MNC	Degree	EPC	Bottleneck	Eccentricity	Closeness	Radiality	Betweenness	Stress	Clustering coefficient
1	C3	Fam20c	Apob	Fn1	Col1a1	Fn1	Fbxo32	Fn1	Fn1	Fn1	Fn1	Oplah
2	Fn1	Mepe	Fn1	Apob	Fn1	Apob	Anapc7	Apob	Apob	Hras	Apob	Slc17a6
3	Fbn1	Fstl3	Fbn1	C3	Msln	Hras	Kctd6	Fbn1	Fstl3	Fbxo32	Fbxo32	Pvalb
4	Timp1	Igfbp5	Col1a1	Fbn1	Fbn1	Fbxo32	Fbxo2	Cp	Cp	Apob	Foxo3	Snrpa
5	Msln	Men1	Col3a1	Col1a1	Col5a1	Mstn	Ubac1	C3	Fbn1	Foxo3	Hras	Iqcb1
6	Apob	Tnc	Col1a2	Timp1	Apob	Fstl3	Asb2	Timp1	Timp1	C3	Fasn	Pde1c
7	Cp	C3	Timp1	Col3a1	Cp	Calm1	Rnf213	Msln	Msln	Cat	Cops5	Ldhd
8	Men1	Col15a1	Msln	Col1a2	C3	Cp	Rbbp6	Fstl3	C3	Mstn	Me1	Cds1
9	Vcan	Col14a1	Col5a2	Cp	Col3a1	Ins2	Lnx1	Men1	Men1	Calm1	Cat	Alcam
10	Fstl3	Anapc7	Col5a1	Msln	Timp1	Srebf1	Fbxo21	Hras	Ctnnb1	Fstl3	Ldhc	Tle1
11	Fam20c	Ubac1	Col2a1	Hras	Tnc	Ceacam1	Rnf7	Vcan	Vcan	Psmb8	Mstn	Ubac1
12	Mepe	Rnf213	Cp	Fbxo32	Col1a2	C3	Ankrd9	Fam20c	Fam20c	Cops5	Cp	Rnf213
13	Igfbp5	Rbbp6	Vcan	Men1	Mepe	Foxo3	Cops5	Mepe	Mepe	Ctnnb1	Fstl3	Rbbp6
14	Tnc	Lnx1	Fam20c	Col5a2	Igfbp5	Fbn1	Myh1	Igfbp5	Igfbp5	Ceacam1	C3	Lnx1
15	Col1a1	Col4a3	Mepe	Col5a1	Col5a2	Cat	Foxo3	Tnc	Tnc	Cp	Xab2	Ank1
16	Col3a1	Col11a1	Fstl3	Col2a1	Col2a1	Pak3	Ring1	Ceacam1	Hras	Fasn	Psmb8	Ankrd9
17	Col1a2	Col5a3	Sparc	Ceacam1	Sparc	Cops5	Mstn	Col1a1	Cat	Anapc7	Aldoc	Fam20c
18	Col5a2	Cp	Igfbp5	Fstl3	Men1	Arfgap1	Prkaa2	Sparc	Ceacam1	Me1	Fbn1	Nek7
19	Col5a1	Vcan	Men1	Vcan	Fam20c	Mapk6	Tnnt2	Col1a2	Foxo3	Espl1	Hnrnpa2b1	Mepe
20	Col2a1	Serpinh1	Tnc	Calm1	Fstl3	Fasn	Casq1	Col3a1	Mstn	Ldhc	Calm1	Rit2

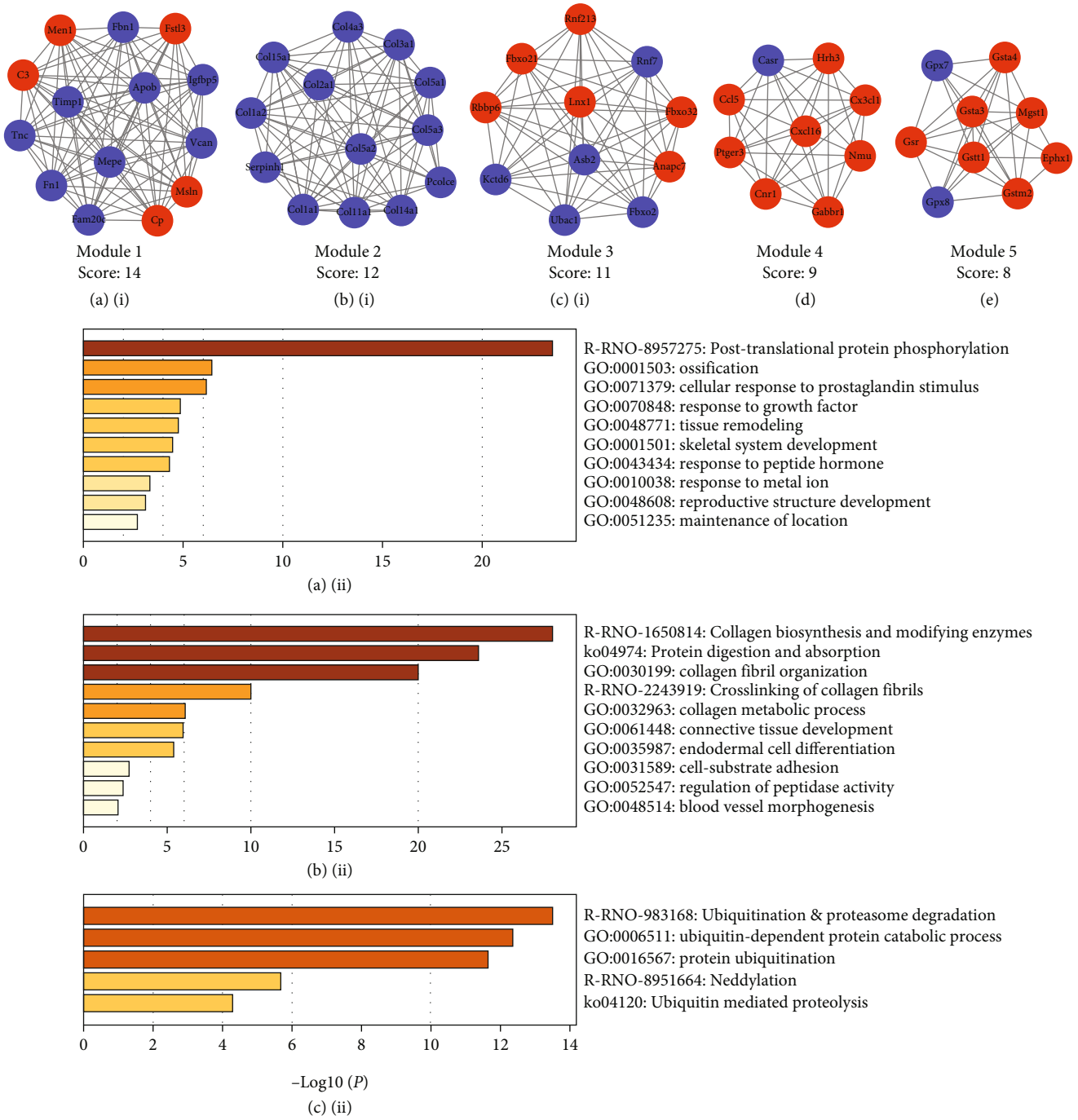

Figure 4: Module analysis of DEGs. Top five modules screened from the PPI network. The genes of the top three modules were performed with enrichment analysis. Nodes are color-coded based on the expression of DEGs (red = upregulated; blue = downregulated). Abbreviations: DEGs: differentially expressed genes; PPI: protein-protein interaction; GO: Gene Ontology.

metabolic process," "purine ribonucleotide metabolic process," "negative regulation of fatty acid metabolic process," and "fatty acid oxidation"; group 4: "regulation of protein secretion"; and group 5: "regulation of ion transport" and "muscle contraction." In Figure 2(c), the network of enriched terms is represented as pie charts, and the colors represent the identities of the gene lists (upregulated or downregulated). Groups 1 and 5 (related to tissue development and structure) mainly represented downregulated DEG pathways, while groups 3 and 4 (related to metabolism pathways) were mainly derived from upregulated DEGs. This is consistent with the results of the clustered heatmap (Figure 1).

3.2. PPI Network, Hub Gene, and Module Analysis. STRING and Cytoscape software were used to detect interactions between the DEGs and construct the PPI network (Figure 3(a)). Considering many DEGs, we set the minimum

NAME	START	SITES	END	STRAND
Fstl3	1116	aaaaaaagaaccaaaaaaaaaaaaaaaaaaa.ag	1084	–
C3	553	aaaaaaaaaaaaaaaaaaaaaaaaaaaaaaa.ac	585	+
Apob	1072	acacacacacacacacacacacacacacacac	1105	+
Men1	41	aaaaaaagaaccaaaaaaaaaaagcactgact.gc	9	–
Fam20c	51	acacagagacagaaacaggtacacacatacacac	18	–
Mepe	1819	agtagaataaacagaaaaataaaaatat.ctcag	1787	–
Fbn1	1990	aaacaaacaaacaaaagaatatccaaag.aacac	1958	–
Igfbp5	1252	acacacacacacacacacacacacacacacacacacac	1285	+
Tnc	774	acatgcagaatgaaaaaaattcccaaag.ct.ac	805	+
Msln	450	aaaaaaaaaaagaaaaagaaaatcacagcctcag	417	–
Timp1	530	acacacacacacacacacacacacacacacacacacac	563	+

Figure 5: Conserved motifs in the promoter sequence of selected genes.

required interaction score to 0.7 to avoid the network being too bloated. In the PPI network, edge color reflects the combined score of the DEGs.

Then, the top 20 hub genes were detected with the cytoHubba plug-in using 12 different algorithms (Table 2). Finally, 16 hub genes, detected by more than six algorithms, were selected to build the hub gene PPI network (Figure 3(b)). Most of the hub genes had a high degree of connectivity. These genes were enriched in "posttranslational protein phosphorylation" and tissue development-related terms (e.g., tissue remodeling, extracellular matrix organization, and skeletal system development) (Figure 3(c)).

MCODE plug-in was used to identify 24 significant modules in PPI network of DEGs. The top five modules were selected for analysis using Metascape. We found that all 14 genes in module 1 belonged to hub genes. Furthermore, module 1 was enriched in posttranslational protein phosphorylation and tissue development-related terms (Figure 4(a)). Notably, the same 11 genes were enriched in "posttranslational protein phosphorylation" term: *Fstl3*, *C3*, *Apob*, *Men1*, *Fam20c*, *Mepe*, *Fbn1*, *Igfbp5*, *Tnc*, *Msln*, and *Timp1*. Thirteen genes belonging to module 2 were enriched in "protein digestion and absorption" and "collagen metabolic remodeling" terms (Figure 4(b)). Module 3 (11 genes) was enriched for the protein ubiquitination process (Figure 4(c)). Genes belonging to module 4 regulated signaling pathways involving G proteins (Figure 4(d) and Figure S2). Module 5 (9 genes) was mainly enriched in "glutathione metabolism" terms (Figure 4(e) and Figure S3).

3.3. Identification of Conserved Motifs in Promoter Site of Genes and Prediction of the Phosphorylation Sites of Protein. Through hub gene and module analysis, we found that the same 11 genes were enriched in the "posttranslational protein phosphorylation" pathway. We speculated that this pathway might play an important role in DED and that these genes may have similar regulatory patterns. Therefore, we used GLAM2 tool to identify common conserved motif upstream of these genes. The consensus sequence AAA (G/C) AAA was observed in the promoter sites of most studied genes (Figure 5). We explored whether the proteins transcribed by these genes had abundant phosphorylation sites. According to the prediction results of NetPhos 3.1 server, most genes, especially *Tnc*, *Fbn1*, *C3*, and *Apob*, have abundant phosphorylation sites (Figure 6).

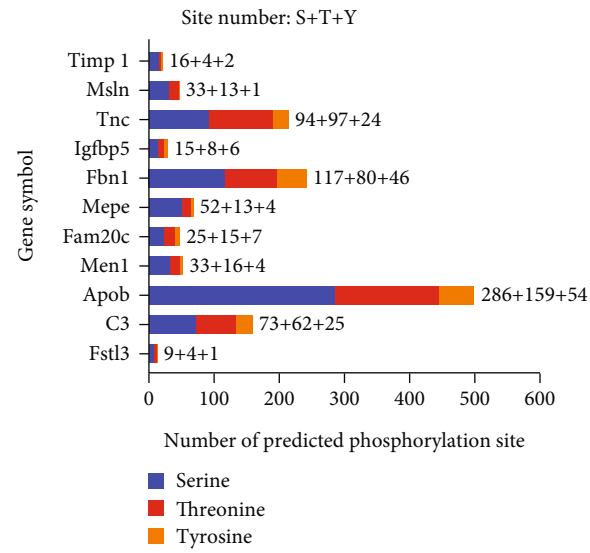

Figure 6: Prediction of phosphorylation sites of proteins transcribed by selected genes.

3.4. Prediction of TFs Associated with DEGs. TFs are important regulators of gene expression. Using ChEA3 tool, we identified 20 TFs that targeted upregulated genes or downregulated genes (Figures 7(a) and 8(a)). The results revealed that TFs related to the upregulated genes were mainly concentrated in "adipose tissue" (Figure 7(b)), "thyroid hormone generation," and "positive regulation of wound healing" (Figure 7(c)). Furthermore, TFs related to downregulated genes were mainly concentrated in "muscle" (Figure 8(b)) and "regulation of skeletal muscle tissue development" (Figure 8(c)).

4. Discussion

Penile erection, a complex neurovascular event, results from the joint action of nerves, blood vessels, and smooth muscles [21]. The main pathophysiology of ED is vascular insufficiency and neuropathy. Diabetes, a metabolic disorder characterized by hyperglycemia, can cause neurological and vascular diseases; therefore, men with diabetes are at risk of ED. Approximately 52.5% of patients with diabetes have ED. Although T2DM is the main type of diabetes, the

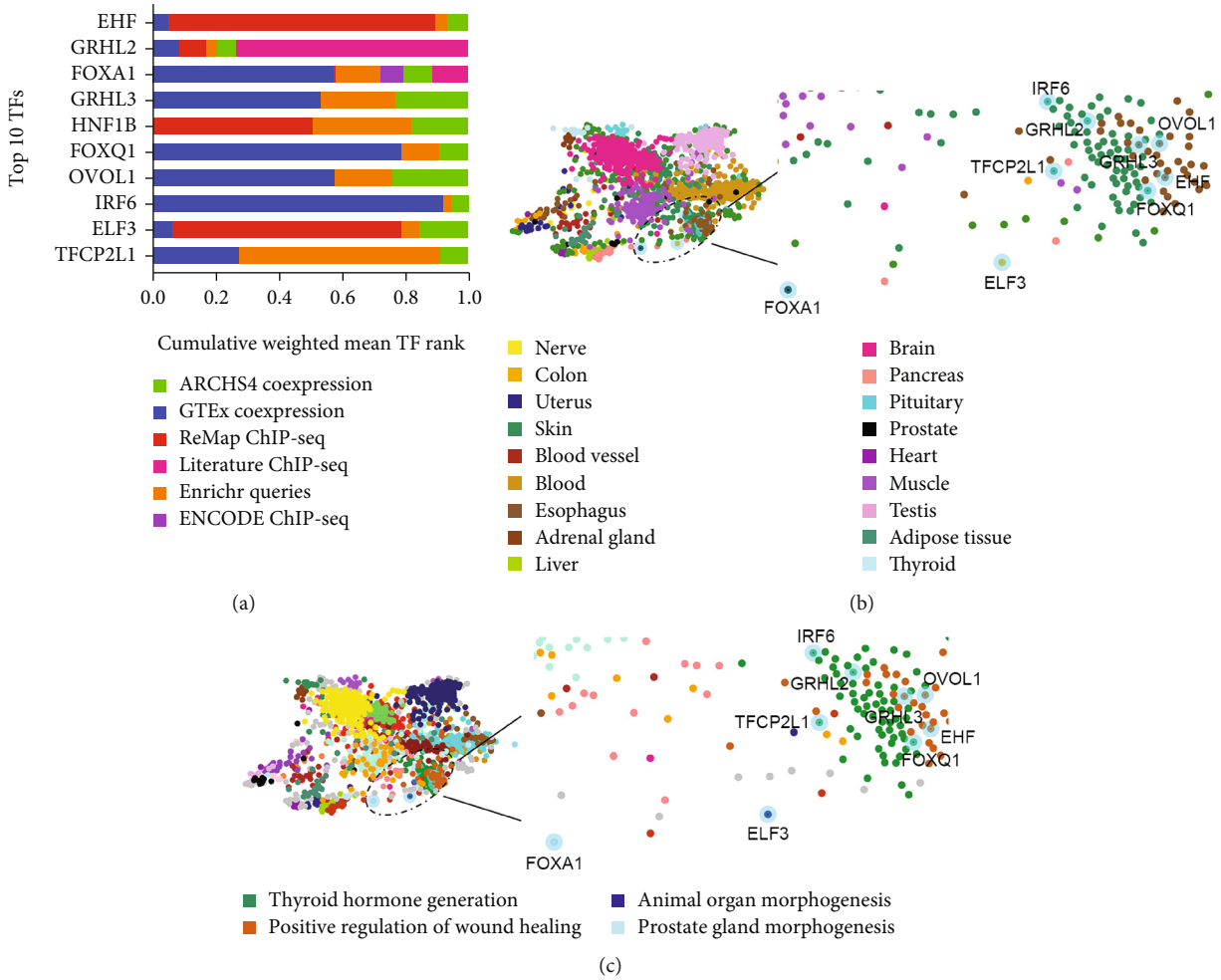

Figure 7: Prediction of TFs related to upregulated genes. (a) Top 10 TFs targeting upregulated genes; (b) tissue locations of predicted TFs; (c) biological functions of predicted TFs. Abbreviations: TFs: transcriptional factors.

incidence of T1DM is increasing worldwide [5, 22]. Existing treatments for ED are not very effective in treating DED. Considering the many diabetic patients, DED places a huge burden on individuals, families, and society. The difficulty of DED treatment is that the pathogenesis is complicated and unclear. Hence, identifying the underlying cellular and molecular mechanisms in DED is important for improving diagnostic and therapeutic strategies.

Although previous studies [13, 23, 24] have reported changes in the gene expression profile of DED cavernous tissues, the methods used in these studies were relatively simple. In this study, we systematically analyzed the molecular correlates leading to DED using bioinformatics analysis. Through the GEO2R tool, 800 DEGs were identified. Changes in the expression of many genes indicate the complexity of DED. To further explore the relationships between them, we performed enrichment analysis, built a PPI network, applied hub genes and module analysis, identified conserved motifs in promoter sites, and predicted the phosphorylation sites. Finally, we predicted TFs associated with DEGs.

The results demonstrated that the upregulated genes were mainly involved in lipid metabolism-related pathways, consistent with the fact that DED patients have diabetes. For example, mitochondrial 3-hydroxy-3-methylglutaryl-CoA synthase (*Hmgcs2*), which catalyzes the first reaction of ketogenesis [25], presented the highest fold change (31.40) in upregulated DEGs. Studies have demonstrated that *Hmgcs2* is closely related to diabetes [26, 27], and inhibiting *Hmgcs2* could alleviate DED [24]. Ceruloplasmin (*Cp*) increased in diabetes [13, 28] and inhibited the activation of endothelial nitric oxide synthase [29].

The downregulated DEGs were primarily enriched in tissue development and structure: "extracellular matrix organization," "muscle contraction," and "skeletal system development." "Extracellular matrix organization" was the most statistically significant term in the enrichment analysis, with 24 downregulated genes. Cellular extracellular matrix plays a key role in developing human organs, maintaining physiological functions, and the onset of disease. Collagen, elastin, and proteoglycan constitute the extracellular matrix of human and rat erectile tissues. The important pathological changes in ED are the apoptosis of cavernous smooth muscle cells, a change in the ratio of smooth muscle to collagen, and atrophy of endothelial cells. Therefore, changes in the composition and structure of the extracellular matrix

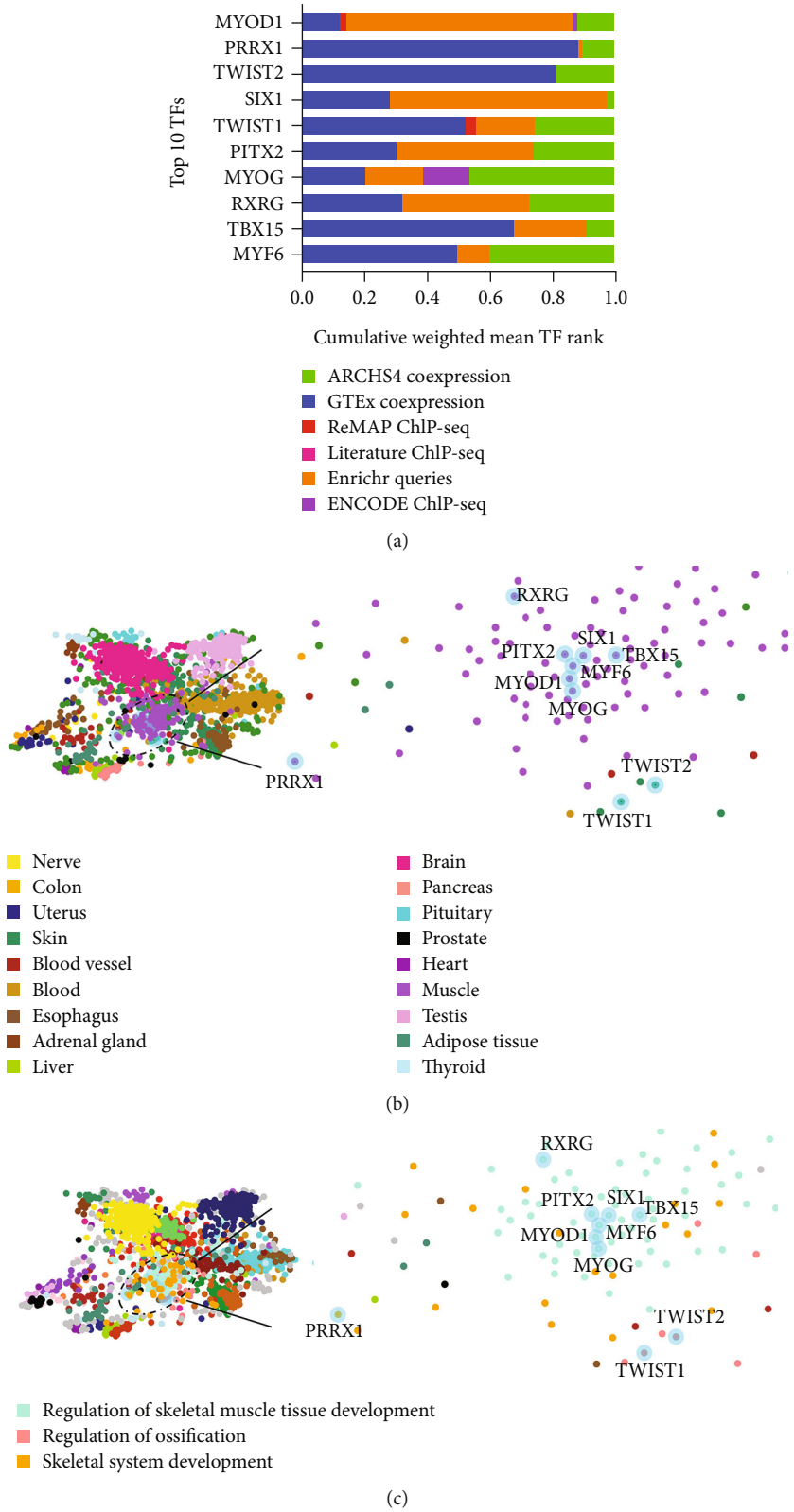

Figure 8: Prediction of TFs related to downregulated genes. (a) Top 10 TFs targeting downregulated genes; (b) tissue locations of predicted TFs; (c) biological functions of predicted TFs. Abbreviations: TFs: transcriptional factors.

caused by diabetes may impair erectile function. The downregulated genes included collagen types 1, 2, 3, 5, 6, 11, 14, and 15. Collagen types 1, 2, 3, 5, and 11 were fibril-forming collagen [30]. Collagen type 1 is the most abundant form of collagen in the erectile tissues of humans and rats and constitutes the framework of the cavernous matrix structure. Collagen 1 is usually formed by two identical a1(I)-chains (*Col1a1*) and one a2(I)-chain (*Col1a2*), which provide tensile stiffness to most organs. In our analysis, both *Col1a1* and *Col1a2* demonstrated decreased expression in DED, which affects the erectile function of the penis. Furthermore, the expression of genes associated with elastic fibers (e.g., Lox [31] and Fbn1 [32]) also decreased. Extracellular matrix mechanical microenvironment regulates cell adhesion, migration, proliferation, and differentiation. Regulating the extracellular matrix structure by stem cells and exosomes is a promising therapeutic strategy for ED. To the best of our knowledge, we built the first enrichment network to demonstrate the relationships between enriched terms. Terms with similar functions were also gathered: groups 1 and 5 were related to tissue development and structure, and groups 3 and 4 were related to metabolic pathways. Altogether, we have depicted the close molecular connections among DEGs.

In PPI network, there were rich interactions between most DEGs. Sixteen hub genes (six upregulated and ten downregulated) were selected using 12 algorithms with the cytoHubba plug-in. These genes were enriched in "post-translational protein phosphorylation" and terms related to tissue development but not in lipid metabolism-related pathways.

MCODE can find and extract closely related regions in PPI network, from which 24 modules were detected. The top five modules were selected for further analysis. Notably, the genes in module 1 (14 genes) belong to hub genes. The module 1 enrichment analysis results were also similar to those of the hub genes. The role of these genes in DED requires further investigation. In addition, we found that "posttranslational protein phosphorylation" was the most statistically significant term for enrichment analysis in module 1 and hub genes, and the same 11 genes were enriched in this term. To verify whether these genes have similar regulatory patterns, we used the GLAM2 tool to identify common conserved motif upstream. In this study, AAA-rich conserved motifs were detected in the promoter site of these genes, which affected the expression patterns by activating and suppressing the transcription of the studied genes. We also found that the proteins transcribed by these genes have abundant phosphorylation sites. Protein phosphorylation is one of the most common and important posttranslational modifications, and it is an important cellular regulatory mechanism [33]. Abnormal protein phosphorylation can be found in many diseases, and the activation or inhibition of this process to treat diseases is theoretically feasible. However, there are relatively few studies on protein phosphorylation during the occurrence and progression of ED. We found that module 2 mainly enriched signatures regarding collagen metabolism, whereas modules 1 and 2 represented downregulated genes. Both the enrichment analyses of hub genes and modules lacked terms regarding glucose and lipid metabolism. Genes related to glucose and lipid metabolism may not play a role in penile lesions but may reflect metabolic disorders of the body, which was demonstrated in patients with DED that had good control of blood glucose levels with progressive ED [34].

TFs are a group of proteins that ensure that target genes are expressed at a specific time and space with a specific intensity and are important regulators of gene expression. We predicted TFs associated with DEGs using the ChEA3 tool. By analyzing the tissue specificity and function of these TFs, we found that TFs targeting upregulated genes were closely related to glucose and lipid metabolism, whereas TFs targeting downregulated genes were more closely related to tissue development. This was consistent with the enrichment results for DEGs. Studies have reported that some of these TFs (e.g., *Foxa1* [35], *ELF3* [36], *Tbx15* [37], *TWIST1*, and *TWIST2* [38]) were involved in diabetes or muscle development. However, the role of these TFs in DED has not been studied.

Although we obtained meaningful results, our study had several limitations. First, sequencing data were obtained from rat samples. Although some genes are conserved among species, these differences cannot be ignored. Therefore, the findings of this study should be verified using human tissues. Cavernous tissue from men undergoing penile surgery or brain-dead male organ donors may provide a viable solution [39]. Second, the genes identified in this study need to be experimentally verified to explore their mechanisms in DED. Third, this study only involved changes in mRNA expression and lacking data on noncoding RNA (miRNAs, lncRNAs, and circRNAs). Noncoding RNA play an important role in the occurrence and development of diabetes and ED [10, 40–42]. The molecular mechanisms of DED can be elucidated by constructing an lncRNA-miRNA-mRNA regulatory network.

5. Conclusions

In this study, we successfully defined the molecular signature of DED. We identified 800 DEGs (407 upregulated and 393 downregulated) in diabetic-induced ED samples. Upregulated DEGs were enriched in glucose and lipid metabolism-related pathways, whereas the downregulated DEGs were primarily enriched in tissue development and structure. Dysregulated extracellular matrix genes (especially collagen and elastin) may be closely related to the damage to the erectile function of the corpus cavernosum. Through hub gene and module analyses, we found some genes that may play a key role in developing DED. Therefore, the role of protein phosphorylation in DED requires further investigation.

Data Availability

The microarray data (GSE2457) supporting this bioinformatics analysis is from previously reported study, which have been cited. The processed data are available in the supplementary files.

Ethical Approval

As all the data in this study were obtained from the GEO public database, approval by the local ethics committee was not required.

Disclosure

The content of the manuscript has been posted as a preprint on Research Square (doi:10.21203/rs.3.rs-1372202/v1) [43].

Conflicts of Interest

The authors declare that they have no competing interests.

Authors' Contributions

Zhiguo Zhu and Xiaoli Li contributed equally to this work and share first authorship. The authors are accountable for all aspects of the work in ensuring that the accuracy or integrity of any part of the work is appropriately investigated and resolved.

Acknowledgments

This work was supported by PhD Research Foundation of Affiliated Hospital of Jining Medical University (2022-BS-001), Jining Key Research and Development Foundation (2021YXNS055), and Guangdong Basic and Applied Basic Research Foundation (2020A1515110946).

Supplementary Materials

Supplementary 1. Table S1: differentially expressed genes were discovered with the GEO2R.

Supplementary 2. Figure S1: heatmap of the top 100 enriched terms across the input gene lists.

Supplementary 3. Figure S2: functional enrichment analysis of module 4.

Supplementary 4. Figure S3: functional enrichment analysis of module 5.

References

[1] F. Hua, "New insights into diabetes mellitus and its complications: a narrative review," *Annals of translational medicine*, vol. 8, no. 24, p. 1689, 2020.

[2] K. Ogurtsova, J. D. da Rocha Fernandes, Y. Huang et al., "IDF Diabetes Atlas: global estimates for the prevalence of diabetes for 2015 and 2040," *Diabetes Research and Clinical Practice*, vol. 128, pp. 40–50, 2017.

[3] X. Zhang, B. Yang, N. Li, and H. Li, "Prevalence and risk factors for erectile dysfunction in Chinese adult males," *The Journal of Sexual Medicine*, vol. 14, no. 10, pp. 1201–1208, 2017.

[4] Y. Kouidrat, D. Pizzol, T. Cosco et al., "High prevalence of erectile dysfunction in diabetes: a systematic review and meta-analysis of 145 studies," *Diabetic Medicine*, vol. 34, no. 9, pp. 1185–1192, 2017.

[5] Y. Xu, Y. Zhang, Y. Yang, L. Liu, Y. Chen, and X. Liu, "Prevalence and correlates of erectile dysfunction in type 2 diabetic men: a population-based cross-sectional study in Chinese men," *International Journal of Impotence Research*, vol. 31, no. 1, pp. 9–14, 2019.

[6] S. Cellek, N. E. Cameron, M. A. Cotter, and A. Muneer, "Pathophysiology of diabetic erectile dysfunction: potential contribution of vasa nervorum and advanced glycation end-products," *International Journal of Impotence Research*, vol. 25, no. 1, pp. 1–6, 2013.

[7] K. Hatzimouratidis and D. Hatzichristou, "How to treat erectile dysfunction in men with diabetes: from pathophysiology to treatment," *Current Diabetes Reports*, vol. 14, no. 11, p. 545, 2014.

[8] L. S. Malavige and J. C. Levy, "Erectile dysfunction in diabetes mellitus," *The Journal of Sexual Medicine*, vol. 6, no. 5, pp. 1232–1247, 2009.

[9] D. Che, Z. Fang, L. Yan et al., "Elevated pigment epithelium-derived factor induces diabetic erectile dysfunction via interruption of the Akt/Hsp90β/eNOS complex," *Diabetologia*, vol. 63, no. 9, pp. 1857–1871, 2020.

[10] W. Huo, Y. Li, Y. Zhang, and H. Li, "Mesenchymal stem cells-derived exosomal microRNA-21-5p downregulates PDCD4 and ameliorates erectile dysfunction in a rat model of diabetes mellitus," *The FASEB Journal*, vol. 34, no. 10, pp. 13345–13360, 2020.

[11] Y. Wen, G. Liu, Y. Zhang, and H. Li, "MicroRNA-205 is associated with diabetes mellitus-induced erectile dysfunction via down-regulating the androgen receptor," *Journal of Cellular and Molecular Medicine*, vol. 23, no. 5, pp. 3257–3270, 2019.

[12] P. Yuan, D. Ma, X. Gao et al., "Liraglutide ameliorates erectile dysfunction via regulating oxidative stress, the RhoA/ROCK pathway and autophagy in diabetes mellitus," *Frontiers in Pharmacology*, vol. 11, p. 1257, 2020.

[13] C. J. Sullivan, T. H. Teal, I. P. Luttrell, K. B. Tran, M. A. Peters, and H. Wessells, "Microarray analysis reveals novel gene expression changes associated with erectile dysfunction in diabetic rats," *Physiological Genomics*, vol. 23, no. 2, pp. 192–205, 2005.

[14] Y. Zhou, B. Zhou, L. Pache et al., "Metascape provides a biologist-oriented resource for the analysis of systems-level datasets," *Nature Communications*, vol. 10, no. 1, p. 1523, 2019.

[15] D. Szklarczyk, A. L. Gable, D. Lyon et al., "STRING v11: protein-protein association networks with increased coverage, supporting functional discovery in genome-wide experimental datasets," *Nucleic Acids Research*, vol. 47, no. D1, pp. D607–D613, 2019.

[16] P. Shannon, A. Markiel, O. Ozier et al., "Cytoscape: a software environment for integrated models of biomolecular interaction networks," *Genome Research*, vol. 13, no. 11, pp. 2498–2504, 2003.

[17] A. D. Yates, P. Achuthan, W. Akanni et al., "Ensembl 2020," *Nucleic Acids Research*, vol. 48, no. D1, pp. D682–D688, 2020.

[18] M. C. Frith, N. F. Saunders, B. Kobe, and T. L. Bailey, "Discovering sequence motifs with arbitrary insertions and deletions," *PLoS Computational Biology*, vol. 4, no. 5, article e1000071, 2008.

[19] N. Blom, T. Sicheritz-Pontén, R. Gupta, S. Gammeltoft, and S. Brunak, "Prediction of post-translational glycosylation and

phosphorylation of proteins from the amino acid sequence," *Proteomics*, vol. 4, no. 6, pp. 1633–1649, 2004.

[20] A. B. Keenan, D. Torre, A. Lachmann et al., "ChEA3: transcription factor enrichment analysis by orthogonal omics integration," *Nucleic Acids Research*, vol. 47, no. W1, pp. W212–W224, 2019.

[21] C. Gratzke, J. Angulo, K. Chitaley et al., "Anatomy, physiology, and pathophysiology of erectile dysfunction," *The Journal of Sexual Medicine*, vol. 7, 1 Part 2, pp. 445–475, 2010.

[22] A. G. Abela and S. Fava, "Why is the incidence of type 1 diabetes increasing?," *Current Diabetes Reviews*, vol. 17, no. 8, article e030521193110, 2021.

[23] S. C. Kam, S. H. Lee, J. H. Jeon et al., "Gene expression profile comparison in the penile tissue of diabetes and cavernous nerve injury-induced erectile dysfunction rat model," *Investigative and clinical urology*, vol. 57, no. 4, pp. 286–297, 2016.

[24] Z. Zhang, H. Y. Zhang, Y. Zhang, and H. Li, "Inactivation of the Ras/MAPK/PPARγ signaling axis alleviates diabetic mellitus-induced erectile dysfunction through suppression of corpus cavernosal endothelial cell apoptosis by inhibiting HMGCS2 expression," *Endocrine*, vol. 63, no. 3, pp. 615–631, 2019.

[25] J. C. Newman and E. Verdin, "Ketone bodies as signaling metabolites," *Trends in Endocrinology and Metabolism: TEM*, vol. 25, no. 1, pp. 42–52, 2014.

[26] G. A. Cook, E. N. Lavrentyev, K. Pham, and E. A. Park, "Streptozotocin diabetes increases mRNA expression of ketogenic enzymes in the rat heart," *Biochimica et Biophysica Acta - General Subjects*, vol. 1861, no. 2, pp. 307–312, 2017.

[27] C. L. Kurtz, B. C. Peck, E. E. Fannin et al., "MicroRNA-29 fine-tunes the expression of key FOXA2-activated lipid metabolism genes and is dysregulated in animal models of insulin resistance and diabetes," *Diabetes*, vol. 63, no. 9, pp. 3141–3148, 2014.

[28] C. Gerhardinger, M. B. Costa, M. C. Coulombe, I. Toth, T. Hoehn, and P. Grosu, "Expression of acute-phase response proteins in retinal Müller cells in diabetes," *Investigative Ophthalmology & Visual Science*, vol. 46, no. 1, pp. 349–357, 2005.

[29] A. Bianchini, G. Musci, and L. Calabrese, "Inhibition of endothelial nitric-oxide synthase by ceruloplasmin," *The Journal of Biological Chemistry*, vol. 274, no. 29, pp. 20265–20270, 1999.

[30] K. Gelse, E. Pöschl, and T. Aigner, "Collagens–structure, function, and biosynthesis," *Advanced Drug Delivery Reviews*, vol. 55, no. 12, pp. 1531–1546, 2003.

[31] Y. L. Song, J. W. Ford, D. Gordon, and C. J. Shanley, "Regulation of lysyl oxidase by interferon-gamma in rat aortic smooth muscle cells," *Arteriosclerosis, Thrombosis, and Vascular Biology*, vol. 20, no. 4, pp. 982–988, 2000.

[32] L. Y. Sakai, D. R. Keene, M. Renard, and J. De Backer, "FBN1: the disease-causing gene for Marfan syndrome and other genetic disorders," *Gene*, vol. 591, no. 1, pp. 279–291, 2016.

[33] F. Ardito, M. Giuliani, D. Perrone, G. Troiano, and L. Lo Muzio, "The crucial role of protein phosphorylation in cell signaling and its use as targeted therapy," *International Journal of Molecular Medicine*, vol. 40, no. 2, pp. 271–280, 2017.

[34] L. Wang, Y. Xu, H. Li et al., "Antioxidant icariside II combined with insulin restores erectile function in streptozotocin-induced type 1 diabetic rats," *Journal of Cellular and Molecular Medicine*, vol. 19, no. 5, pp. 960–969, 2015.

[35] M. Z. Vatamaniuk, R. K. Gupta, K. A. Lantz, N. M. Doliba, F. M. Matschinsky, and K. H. Kaestner, "Foxa1-deficient mice exhibit impaired insulin secretion due to uncoupled oxidative phosphorylation," *Diabetes*, vol. 55, no. 10, pp. 2730–2736, 2006.

[36] M. Lopes, B. Kutlu, M. Miani et al., "Temporal profiling of cytokine-induced genes in pancreatic β-cells by meta- analysis and network inference," *Genomics*, vol. 103, no. 4, pp. 264–275, 2014.

[37] K. Y. Lee, M. K. Singh, S. Ussar et al., "Tbx15 controls skeletal muscle fibre-type determination and muscle metabolism," *Nature Communications*, vol. 6, no. 1, p. 8054, 2015.

[38] J. M. Mudry, J. Massart, F. L. Szekeres, and A. Krook, "TWIST1 and TWIST2 regulate glycogen storage and inflammatory genes in skeletal muscle," *The Journal of Endocrinology*, vol. 224, no. 3, pp. 303–313, 2015.

[39] H. Wessells, C. J. Sullivan, Y. Tsubota et al., "Transcriptional profiling of human cavernosal endothelial cells reveals distinctive cell adhesion phenotype and role for claudin 11 in vascular barrier function," *Physiological Genomics*, vol. 39, no. 2, pp. 100–108, 2009.

[40] R. Cong, Y. Wang, Y. Wang et al., "Comprehensive analysis of lncRNA expression pattern and lncRNA-miRNA-mRNA network in a rat model with cavernous nerve injury erectile dysfunction," *The Journal of Sexual Medicine*, vol. 17, no. 9, pp. 1603–1617, 2020.

[41] F. Peng, W. Gong, S. Li et al., "circRNA_010383 acts as a sponge for miR-135a, and its downregulated expression contributes to renal fibrosis in diabetic nephropathy," *Diabetes*, vol. 70, no. 2, pp. 603–615, 2021.

[42] W. Ying, H. Gao, F. C. G. Dos Reis et al., "MiR-690, an exosomal-derived miRNA from M2-polarized macrophages, improves insulin sensitivity in obese mice," *Cell Metabolism*, vol. 33, no. 4, pp. 781–790.e5, 2021.

[43] Z. Zhu, X. Li, X. Cao et al., "Identification and characterization of the gene profile in diabetes induced erectile dysfunction rat model," *Research Square*, 2022.